PCCP

COMMUNICATION

View Article Online
View Journal | View Issue

Cite this: *Phys. Chem. Chem. Phys.*, 2014, **16**, 19841

Received 27th July 2014,
Accepted 30th July 2014

DOI: 10.1039/c4cp03329a

www.rsc.org/pccp

Degradation mechanism of sulfonated poly(ether ether ketone) (SPEEK) ion exchange membranes under vanadium flow battery medium†

Zhizhang Yuan,[ab] Xianfeng Li,*[a] Jinbo Hu,[c] Wanxing Xu,[ab] Jingyu Cao[ab] and Huamin Zhang*[a]

The degradation mechanism of hydrocarbon ion exchange membranes under vanadium flow battery (VFB) medium was investigated and clarified for the first time. This work will be highly beneficial for improving the chemical stability of hydrocarbon ion exchange membranes, which is one of the most challenging issues for VFB application.

Concerns over fossil energy shortages and environmental load are driving forces for the research efforts into renewable energies like solar and wind power. However, the intermittent and random nature of these renewable energies seriously affects the final quality of the output electricity as well as their stability in the grid. Electric energy storage (EES) has become a valid solution to solve these problems.[1] Combined with renewable energies, energy storage can increase the quality and stability of photovoltaic (PV) and wind-generated electricity.[2] As one kind of energy technique, vanadium flow batteries (VFBs) have emerged as a promising alternative to existing large-scale power conversion systems, due to their perfect combination of high energy efficiency, high safety and reliability.[3–5] VFBs, originally proposed by Maria Skyllas-Kazacos in 1985, are composed of two tanks filled with an active species of vanadium ions in different valance states, two pumps and a battery cell. The conversion between electrical and chemical energy is realized by the reduction and oxidation of the vanadium ions.[5,6] Although vast demonstrations of VFBs in different fields have been accomplished, there is still an urgent need for the development of high-quality and low-cost membranes, which are believed to be vital to achieve cost effective VFB systems.[7–14]

Perfluorinated cation exchange membranes, such as DuPont's Nafion series[4,15] are the most commonly used membranes in VFBs due to their superior proton conductivity and chemical stability. However, their low ion selectivity and extremely high cost have hindered their application in the commercialization of VFBs.[2] Hydrocarbon ion exchange membranes such as sulfonated polyaromatic polymers (sulfonated poly(aryl ketone ketone), poly(aryl ether sulfone), polyimide *etc.*) are the most studied systems due to their tunable ion conductivity and low cost.[12,16] However, these membranes suffer from low chemical stability in VFB medium. The degradation mechanism of the hydrocarbon ion exchange membranes has been unclear, since the medium of VFB is very complicated (strongly acidic, oxidizing and with high electric potential). Quite recently, Hickner *et al.* proposed a mechanism of sulfonated poly(sulfone) (S-Radel) degradation behavior in a solution of V(v), where the reactive species first attack the S-Radel by incorporating hydroxyl groups into the polymer backbone and then oxidize them into quinone functionalities.[17] Fujimoto *et al.* investigated the chemical stability of sulfonated Diels–Alder poly(phenylene) (SDAPP) with different ion exchange capacities (IECs), showing that the degradation was accelerated with increasing content of ion exchange groups.[18] In spite of these reports, studies of degradation mechanisms are very limited and the detailed degradation reaction of membranes under VFB medium is not clear, leading to very few relevant strategies for synthesizing new materials with excellent performances for VFB application.[19] Therefore, there is an urgent need to clarify the degradation mechanism of sulfonated hydrocarbon membranes under VFB operating conditions, which would open up a new perspective for designing more durable and economically viable membranes, and would further accelerate VFB commercialization.

In this study, with an aim to understand the degradation of hydrocarbon ion exchange membranes, we chose sulfonated poly(ether ether ketone) (SPEEK) membranes with different DS as model materials (Scheme 1), where DS is the number of sulfonated groups per repeating unit. The influence of the ion exchange group ($-SO_3H$) on oxidation stability during *ex situ* testing was investigated.

[a] *Division of Energy Storage, Dalian Institute of Chemical Physics, Chinese Academy of Sciences, Zhongshan Road 457, Dalian 116023, China. E-mail: lixianfeng@dicp.ac.cn, zhanghm@dicp.ac.cn*
[b] *University of Chinese Academy of Sciences, Beijing 100039, China*
[c] *Key Laboratory of Organofluorine Chemistry, Shanghai Institute of Organic Chemistry, Chinese Academy of Sciences, 345 Ling-Ling Road, Shanghai, 200032, China*

† Electronic supplementary information (ESI) available: Experimental section; NMR, FTIR, SEM, LC-MS spectra; fragment ion peaks. See DOI: 10.1039/c4cp03329a

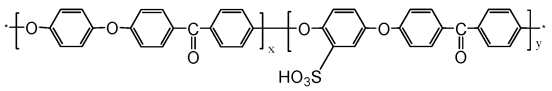

Scheme 1 The chemical structure of SPEEK.

Table 1 Physical properties of SPEEK membranes

Membrane	Thickness (μm)	DS	Water uptake (%)	Swelling (%)
SP1	100 ± 5	0.74	49.85	20.00
SP2	100 ± 5	0.84	67.18	25.00
SP3	100 ± 5	0.91	70.27	27.66

To clarify the degradation mechanism, the chemical structure of the degradation products (both from *ex situ* and *in situ* experiments) was further analyzed and confirmed by LC-MS.

To fully understand the role of the ion exchange groups on the oxidation stability of the membranes, SP1, SP2 and SP3 membranes with different DS were fabricated for further investigation. The chemical structures were determined by ^{1}H NMR (Fig. S1 of ESI†) and the basic physical parameters of the membranes are shown in Table 1. With increasing DS, a regular rise of water uptake and swelling rate can be observed. This can be attributed to the sulfonic acid functional groups, leading to hydrophilic water channels, which result in higher water uptake and swelling behavior.

To confirm the relationship between oxidation stability and the amount of sulfonic acid functional groups, SP1, SP2 and SP3 membranes with a fixed size (4 cm × 4 cm) were immersed in 0.15 M VO_2^+ to detect the concentration changes of VO^{2+}, which are induced by SPEEK degradation. Obvious color changes (Fig. S2, ESI†) were detected in 0.15 M VO_2^+ solutions containing SPEEK membranes (40 °C) after 30 days. In contrast, the color of the solution containing the SPEEK membranes turned green as a result of the reduction of VO_2^+ to VO^{2+}, indicating that the membranes were gradually oxidized by VO_2^+. The VO^{2+} concentration in the solutions increased with increasing DS (Fig. 1), suggesting that the oxidation stability of the membranes decreases with increasing DS, or that the sulfonic acid groups accelerate the degradation of the membranes. This can possibly be explained by the fact that the membrane with a higher DS resulted in higher swelling, generating hydrophilic channels within the hydrophobic matrix. This in turn promotes the absorption of VO_2^+ and induces membrane oxidation, resulting from contact between the polymer chains and VO_2^+.

To further investigate the membrane degradation mechanism, the concentration of VO_2^+ was increased to 1.5 M to accelerate the membrane degradation. After a 30 h immersion, SP3 with the highest DS was broken into pieces (Fig. S3, ESI†), while SP1 and SP2 remained intact, further confirming the role of the sulfonated groups. The surface and cross-sectional morphology of the membranes after VO_2^+ treatment was detected using SEM. All the membranes were cracked after soaking in 1.5 M VO_2^+ at 40 °C for 30 h, as shown in the surface SEM images (Fig. 2), and they became thinner after degradation. In addition, with increasing DS, the surface cracks became more serious,

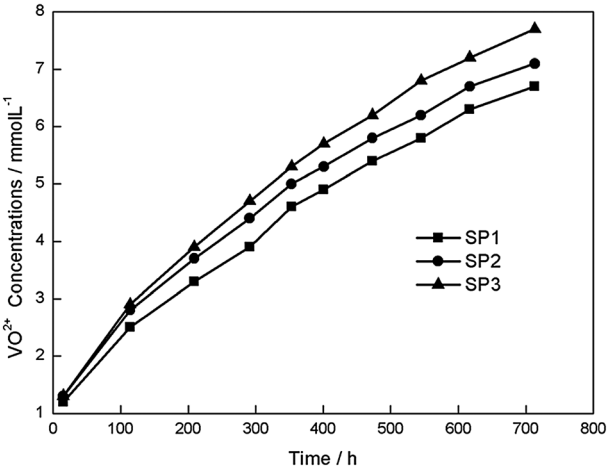

Fig. 1 The change in VO^{2+} concentration in electrolyte solutions (0.15 M VO_2^+ in 3 M total sulfate) containing SPEEK membranes at 40 °C, as a function of time.

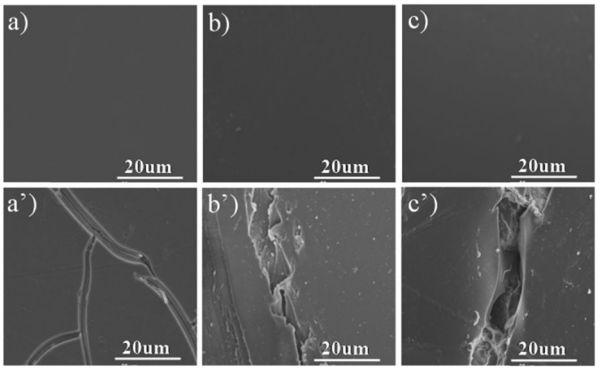

Fig. 2 SEM micrographs of the membrane surface before: (a) SP1, (b) SP2, and (c) SP3, and after: (a′) SP1, (b′) SP2, and (c′) SP3, immersion in 1.5 M VO_2^+ at 40 °C for 30 h.

indicating that the introduction of sulfonic acid functional groups accelerated the degradation of the membranes. The cross-sectional SEM images of the original membranes and the degraded membranes were detected as well (Fig. 3). Compared to the original membranes, micro-pores were clearly formed (Fig. 3) after soaking in 1.5 M VO_2^+ at 40 °C for 30 h. Similar to previously reported results,[20] the SP3 membrane even suffers from a grievous delaminating process, where small pieces of the membrane break away from the sample (Fig. 3).

To clarify the degradation mechanism of the SPEEK membranes during *ex situ* tests, the SP3 membrane was selected to investigate the chemical structure of the degradation products. Fig. 4a and b show the ^{1}H NMR spectra of the initial SP3 membrane, and the SP3 membrane after it is immersed in 1.5 M VO_2^+ for 30 hours, respectively. Compared to the initial SP3 membrane, no significant differences could be found in the full ^{1}H NMR spectrum, except for the new aromatic proton peaks that emerged at around 6.9 ppm and 7.7 ppm after degradation, suggesting that no aliphatic carbons were produced during *ex situ* degradation. In addition to this, the chemical shift and

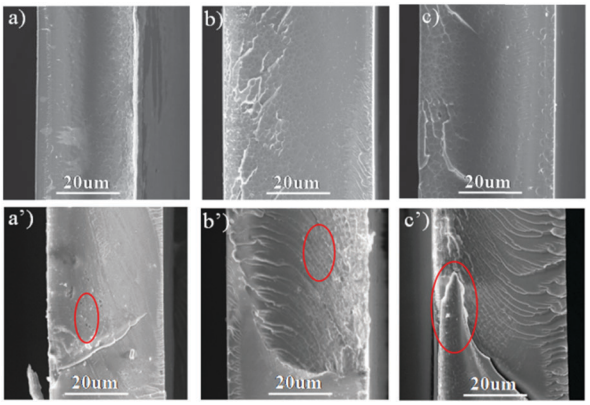

Fig. 3 SEM micrographs of the membrane cross-section before: (a) SP1, (b) SP2, and (c) SP3, and after: (a′) SP1, (b′) SP2, and (c′) SP3, immersion in 1.5 M VO_2^+ at 40 °C for 30 h.

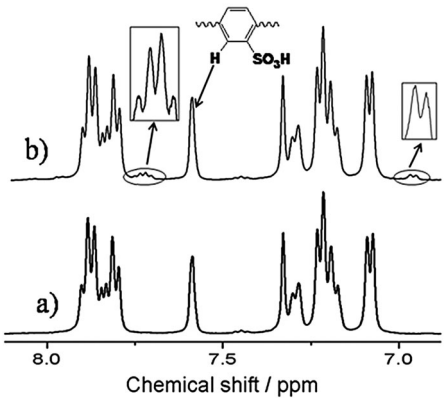

Fig. 4 ^{1}H NMR spectra of the initial SP3 membrane (a) and the degraded SP3 membrane (b) in DMSO-d_6.

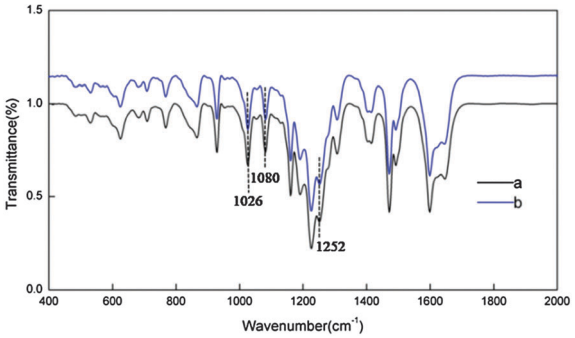

Fig. 5 FTIR spectra of the initial SP3 membrane (a) and the degraded SP3 membrane (b).

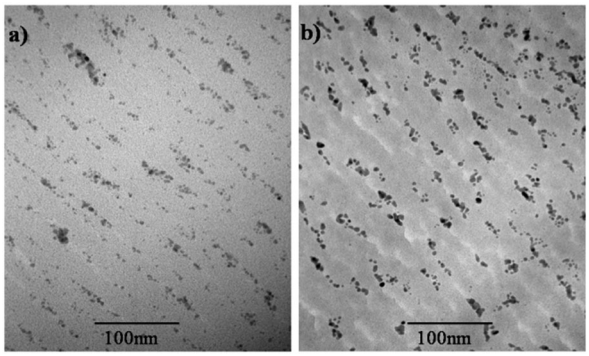

Fig. 6 Distribution of $-SO_3H$ in the initial SP3 membrane (a) and the degraded SP3 membrane (b).

signal intensity (Fig. 4) of the *ortho* hydrogen atoms of the sulfonic acid group did not change obviously before and after degradation, suggesting that the sulfonic acid functional groups remained unchanged after degradation. This conclusion is very different from the reported sulfonated polysulfone, where the sulfonate groups experienced some chemical degradation as well.[20]

FTIR was employed to confirm the chemical structure of the initial and degraded SP3 membranes. The FTIR results are displayed in Fig. 5. Peaks at 1026 cm^{-1} and 1080 cm^{-1} are attributed to the asymmetric and symmetric stretching of the S=O bond from the sulfonic acid functional groups, for both the initial (a) and the degraded (b) SP3 membranes, again confirming that the sulfonic acid functional groups remained stable during *ex situ* degradation. The full FTIR spectra did not show any obvious differences between the initial and degraded SP3 membranes, again indicating that no aliphatic carbon was formed during *ex situ* testing.

TEM was performed on the initial SP3 and degraded SP3 membranes after staining with 1 M $AgNO_3$ to detect the distribution of the sulfonic acid functional groups. The dark spots on the initial and degraded membranes shown in Fig. 6a and b are attributed to the clusters formed by the interaction between Ag^+ and the negatively charged sulfonic acid groups of the membrane, indicating that the sulfonic acid functional groups remained unchanged after degradation.

The ^{1}H NMR and TEM results indicate that the polymer backbone experienced grievous chain rupture while the sulfonic acid functional groups remained stable. However, the new aromatic peaks shown in Fig. 4b emerged at a relatively low intensity, and were very difficult to assign due to the complex random polymer. To further identify the chemical structure of the degradation products, the immersion time was prolonged to 54 h to degrade the membranes into shorter chains. As expected, the SP3 membrane was broken up into small pieces after treatment. Furthermore, we were surprised to find that the degradation products with smaller molecular weights became water soluble (Fig. S4, ESI†), indicating the existence of sulfonic acid groups.

To further identify the chemical structure of the degradation products, LC-MS was employed to detect their molecular weights. The full LC-MS spectrogram of the aqueous solution with a negative mode is rather complicated and is shown in Fig. S5 (ESI†). However, some major characteristic fragment ion peaks can be recognized and identified as the structures shown in Scheme 2.

Judging from these fragment ion peaks, we can draw a conclusion that the polymer backbone was broken from the

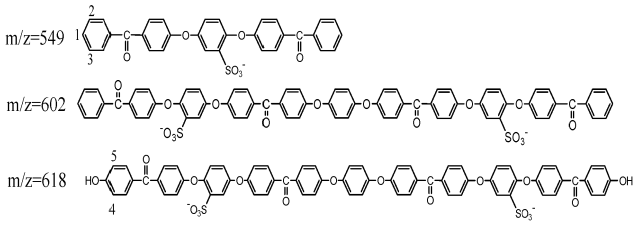

Scheme 2 Parts of the fragment ion peaks obtained by LC-MS.

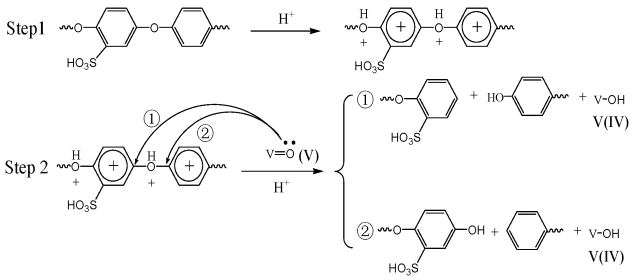

Scheme 3 The degradation mechanism of the SP3 membrane during *ex situ* testing.

ether bond, while leaving the sulfonic acid functional groups stable. The structure of the degradation products can well explain the new aromatic peaks which emerged, and are shown in Fig. 4b. After the ether bond cracked, new aromatic hydrogens, such as H1 shown in Scheme 2, appeared. H1, H2, and H3, shown in Scheme 2, are quadruple peaks, while H4 and H5 are double peaks in the ^{1}H NMR spectra, and perfectly match the new peaks which emerged in the ^{1}H NMR spectra (Fig. 4) after 30 h degradation.

^{1}H NMR was performed on the degraded SP3 membrane after immersion in 1.5 M VO_2^+ for 54 h as a comparison. Surprisingly, the chemical shift and signal intensity of the new aromatic peaks shown in Fig. 4b have not increased so much, while obvious changes have taken place on the main peaks, as shown in Fig. 7. This provides further evidence that the polymer backbone experienced grievous chain scission. Apart from this, a new peak at around 5.0 ppm has clearly emerged, which can be assigned to the complexation of –OH, further supporting the breakage of the ether bond. There was no significant difference between the initial and the degraded SP3 membranes (soaking in 1.5 M VO_2^+ for 30 h and 54 h) in the ^{13}C NMR spectra (Fig. S6–S8, ESI†), again indicating that no aliphatic carbon was formed during the degradation.

Based on the above results, the degradation mechanism of the SPEEK membrane can be proposed as shown in Scheme 3. Under the strong acidic conditions, the ethereal oxygen atoms in SPEEK could be easily protonated and become strong electron-withdrawing groups. The protonated ether functionality together with the strong electron-withdrawing sulfonic acid group induce a strong electrophilic carbon center on the benzene ring, which can be easily attacked by the lone pair electron on the vanadium(v) oxygen species. According to a previous report,[17] membranes soaked in $VOCl_3$ exhibit no degradation during *ex situ* testing, which offers important information that the acidic medium greatly promotes vanadium(v) ion oxidation. This can be explained by the theory of contrapolarization.[21,22] The charge at the center of the vanadium(v) atom in the vanadium(v) oxygen species is very high, leading to a strong polarization effect, which in turn results in deformation of the oxygen electron clouds, making the oxygen close to vanadium(v) electronegative. While under the strong acidic medium, H^+ was almost a naked proton, and has a very strong attraction for the electron cloud, resulting from its extremely high positive charge density. The polarization of oxygen resulting from H^+ and vanadium(v) is opposite, known as contrapolarization. The contrapolarization effect of H^+ makes the oxygen close to H^+ electronegative and the oxygen close to vanadium(v) electropositive, weakening the covalent bond between the vanadium(v) and oxygen atoms. This contrapolarization effect makes breaking of the covalent bond easier, further facilitating the reduction of VO_2^+ to VO^{2+}.

To support the mechanism we proposed above, SP3 membranes were immersed in 0.15 M VO_2^+ solutions with different concentrations of sulfuric acid (1 M, 2 M, and 3 M) to clarify the role of protonation. As shown in Fig. 8, with increasing acid concentration, the concentration of VO^{2+} reduced from VO_2^+ increases and the degradation becomes more serious, further confirming our assumptions.

The degradation mechanism of the above *ex situ* tests may differ from the practical degradation process in VFBs since some dynamic factors are ignored, especially the high

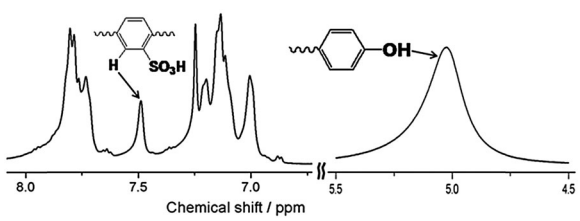

Fig. 7 ^{1}H NMR spectrum of the SP3 membrane after soaking in 1.5 M VO_2^+ for 54 h.

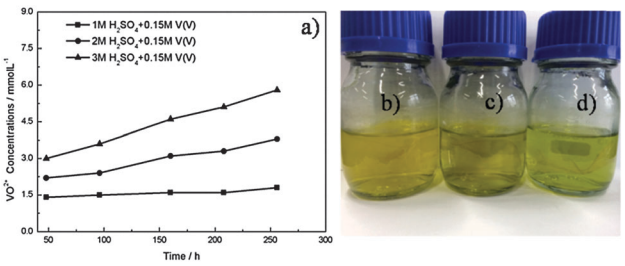

Fig. 8 Influence of protonation on membrane oxidation stability: (a) VO^{2+} concentration change containing SP3 membranes at 40 °C as function of time; (b) SP3 membrane + 1 M H_2SO_4 + 0.15 M VO_2^+; (c) SP3 membrane + 2 M H_2SO_4 + 0.15 M VO_2^+; (d) SP3 membrane + 3 M H_2SO_4 + 0.15 M VO_2^+.

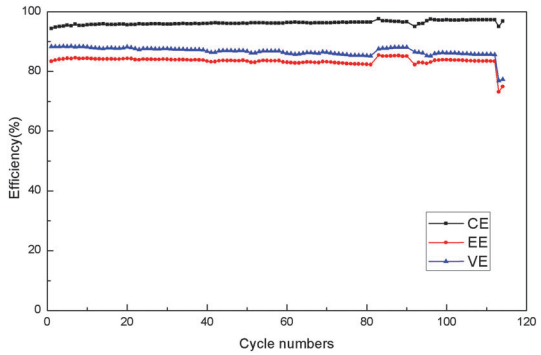

Fig. 9 The on-line cycle performance of a VFB assembled with SP3 membranes.

potential. Therefore, an *in situ* online test was carried out *via* a single VFB cell cycling test. A VFB assembled with SP3 membranes shows CE, EE and VE values of 96%, 84% and 88% at a current density of 80 mA cm^{-2}, which is a bit higher than commercialized Nafion115.[23] However, the performance suddenly dropped after continuously running for more than 100 cycles (Fig. 9).

SEM was employed to investigate the change in membrane morphology after a lifetime test. In Fig. 10a, the membrane facing the positive half-cell was covered with cracks and pores, while the membrane facing the negative half-cell exhibited no significant changes as shown in Fig. 10b, indicating that the VO_2^+ ions existing in the positive electrolyte serve as the main source that induces the degradation of the membrane. Fig. 10c shows the cross-section of SP3 membrane after cycle life test, inner pores are generated throughout the membrane as a result of the membrane degradation. The edge of the membrane facing the positive half-cell has already cracked as marked in red line in Fig. 10c.

For comparison, a ^1H NMR study was also carried out on the SP3 membrane after a lifetime test (Fig. 11). Compared to the degradation products of the SP3 membrane from the *ex situ* test, overall, the ^1H NMR spectra of the SP3 membrane after the lifetime test showed the same peaks for the membranes soaked in 1.5 M VO_2^+ for 30 h (Fig. 11a). The same new aromatic peaks also emerged in the ^1H NMR spectra after the lifetime test. The results showed that the structure of the degradation products after the cycling test is the same as that during *ex situ* degradation. The existence of an electric field will not affect the degradation mechanism of the membranes

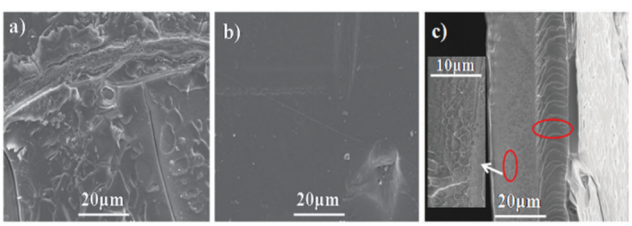

Fig. 10 SEM micrographs of SP3 membrane surface after lifetime test: (a) facing positive half-cell; (b) facing negative half-cell; (c) cross-section after lifetime test.

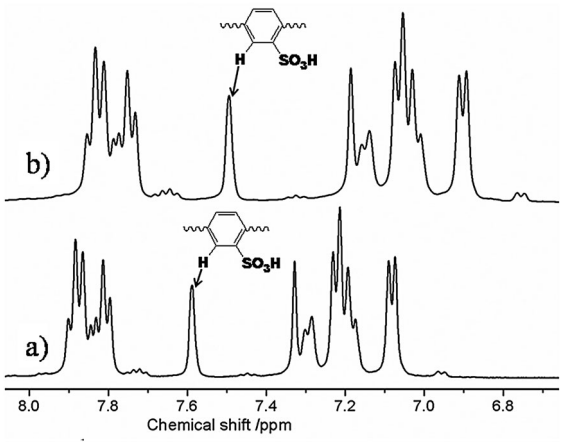

Fig. 11 ^1H NMR spectra of the SP3 membrane: (a) when soaked in 1.5 M VO_2^+ for 30 h and (b) after a lifetime test.

under VFB operating conditions, indicating the availability of the *ex situ* oxidation stability test. Furthermore, the chemical shift of the SP3 membrane after the cycling test moves to the high field, as shown in Fig. 11b. This can be explained by the different vanadium ions that exist in the membranes. For the *ex situ* test, VO_2^+ ions are adsorbed by the membranes, while under the VFB charge/discharge test the VO^{2+} ions are reported to be the most adsorbed ions in the membranes.[24,25] The interaction between the sulfonic acid groups and the different vanadium ions possibly induces different chemical shifts.

Conclusions

SPEEKs with different DS were prepared and selected as model compounds to investigate the degradation mechanism of hydrocarbon membranes under VFB operating conditions. The degradation mechanism was proposed clearly for the first time, and was supported by experimental data. According to the proposed mechanism, apart from the sulfonic acid groups, the protonation of ethereal oxygen atoms under strong acid medium plays very important roles in accelerating membrane degradation. Therefore, strategies such as protecting the ether bond, synthesising new compounds without an ether bond, or introducing electron-donating groups to the aromatic backbone, could be very effective for improving the oxidation stability of the membrane for VFB applications.

Experimental

Materials and methods

Materials. Poly(ether ether ketone) was kindly provided by Changchun Jilin University Special Plastic Engineering Research. The 1.5 M VO_2^+ in 3.0 M total sulfate solution was prepared by oxidation of 1.5 M $VOSO_4$ + 1.5 M H_2SO_4. The 0.15 M VO_2^+ in 3.0 M total sulfate solution was prepared by diluting the 1.5 M VO_2^+ in 3.0 M total sulfate solution with sulfuric acid according to the

literature.[20] All the other chemicals were used as received without further purification.

Membrane preparation. SPEEK polymers with various DS were prepared by direct sulfonation of PEEK with sulfuric acid at 40 °C for 6 h, 9 h and 10.5 h, as described elsewhere.[26] The degree of sulfonation, which was determined by ^{1}H NMR,[27] is in the range between 0.74 and 0.91 and is referred to as SP1, SP2 and SP3. The SPEEK membranes were cast from 25 wt% *N*,*N*-dimethylacetamide (DMAc) solutions and dried. Afterwards, the membranes were peeled off and the thickness of the membranes was 100 ± 5 μm. To detect the water uptake and swelling of the membranes, the membranes were first soaked in deionized water for 3 days in order to saturate them with water. The weight of the saturated membranes was then obtained after quickly wiping off the surface water using a tissue. The water uptake is defined as the weight ratio of the absorbed water to the dry membrane, as shown in eqn (1):

$$\text{Water uptake}(\%) = \frac{W_s - W_d}{W_d} \times 100 \quad (1)$$

where W_s and W_d are the weights of the saturated and dry membranes, respectively.

The swelling is defined as the length ratio of the swollen membranes to the dry membranes, as shown in eqn (2):

$$\text{Swelling}(\%) = \frac{L_s - L_d}{L_d} \times 100 \quad (2)$$

where L_s and L_d are the lengths of the saturated and dry membranes, respectively.

***Ex situ* oxidation stability test.** To investigate the influence of the ion exchange groups on the oxidation stability of the membranes, SPEEK membranes with a fixed size (4 cm × 4 cm) were soaked in 60 ml electrolyte solution (0.15 M VO_2^+ in 3 M total sulfate) in sealed glass vials at 40 °C. During the test, 4 ml of electrolyte was collected from each vial at a regular time interval and the VO^{2+} concentration in the electrolyte samples was detected using UV-Vis. To better understand the degradation mechanism, SP3 with the highest DS was selected as an example, a more concentrated VO_2^+ solution (1.5 M VO_2^+ in 3 M total sulfate) was used to accelerate the membrane degradation, and the degradation products were further analyzed. The immersion time was kept at 30 and 54 h.

"On-line" or *in situ* VFB cycle life test. For comparison, an on-line cycle life test was carried out on SP3 *via* a VFB single cell test as well. Detailed information on the VFB assembly was reported previously.[28] A VFB single cell was assembled by sandwiching a membrane with two carbon felt electrodes, clamped by two graphite polar plates. All these components were fixed between two stainless plates. 30 ml 1.5 M VO^{2+}/VO_2^+ in 3.0 M H_2SO_4 and 30 ml 1.5 M V^{2+}/V^{3+} in 3.0 M H_2SO_4 were used as the positive and negative electrolytes respectively. The electrolyte was cyclically pumped through the corresponding electrodes in airtight pipelines. Charge–discharge cycling tests were conducted using ArbinBT2000 with a constant current density of 80 mA cm^{-2}. The cut-off voltage for discharge and charge was set at 0.8 V and 1.65 V respectively, to avoid the corrosion of the carbon felts and graphite polar plates. After the cycle test, the composition of the membrane structure was analyzed in detail.

Characterization. ^{1}H NMR and ^{13}C NMR spectra were recorded on a BRUKER DRX400 using DMSO-d_6 as the solvent and tetramethylsilane (TMS) as the internal standard. A UV-Vis spectrometer (JASCO, FT-IR 4100, Japan) was used to determine the concentration of VO^{2+}. Ultra-High Definition (UHD) Accurate-Mass Q-TOF LC-MS was performed using an Agilent 6540 Q-TOF to determine the degradation products with a negative mode. The instrument parameters are as follows; gas temperature: 325 °C; flow rate of drying gas: 8 L min^{-1}; Nebulizer: 25 psig; VCap: 3500 V; fragmentor: 175 V; skimmer: 65 V; OCT: 1 RF; Vpp: 750 V; mass range: 50–1700. The distribution of the negatively charged groups (–SO_3H) in the membrane samples before and after degradation were recorded using TEM (JEM-2000EX, JEOL). All the prepared membrane samples were dyed with 1 M silver nitrate solution and then washed with deionized water to remove the silver ions absorbed in the membrane. After that, the membranes were dried and then fixed in epoxy before being cut into thin slice samples. Fourier transformed infrared spectroscopy (FTIR) (Avatar.370 E.S.P., Nicolet Continuum Infrared Microscope) was used to determine the chemical structure of the membranes before and after degradation. The membrane samples were first dissolved in DMAc to form a 4 wt% solution and then cast onto a KBr crystal. The KBr crystal was then dried at 60 °C under ambient pressure for 12 h, followed by drying under a vacuum for 24 h at 80 °C. The cross-sectional and surface morphologies were detected by SEM (JEOL 6360LV, Japan) with an acceleration voltage of 10 kV. The cross-sections were obtained by breaking the membranes in liquid nitrogen and coating them with gold prior to imaging.

Notes and references

1 B. Dunn, H. Kamath and J.-M. Tarascon, *Science*, 2011, **334**, 928–935.
2 X. Li, H. Zhang, Z. Mai, H. Zhang and I. Vankelecom, *Energy Environ. Sci.*, 2011, **4**, 1147–1160.
3 H. Zhang, H. Zhang, X. Li, Z. Mai and J. Zhang, *Energy Environ. Sci.*, 2011, **4**, 1676–1679.
4 M. Skyllas-Kazacos, M. Chakrabarti, S. Hajimolana, F. Mjalli and M. Saleem, *J. Electrochem. Soc.*, 2011, **158**, R55–R79.
5 M. Skyllas-Kazacos, M. Rychcik, R. G. Robins, A. Fane and M. Green, *J. Electrochem. Soc.*, 1986, **133**, 1057–1058.
6 C. Ponce de León, A. Frías-Ferrer, J. González-García, D. A. Szánto and F. C. Walsh, *J. Power Sources*, 2006, **160**, 716–732.
7 T. Sukkar and M. Skyllas-Kazacos, *J. Membr. Sci.*, 2003, **222**, 249–264.
8 Q. Luo, H. Zhang, J. Chen, P. Qian and Y. Zhai, *J. Membr. Sci.*, 2008, **311**, 98–103.
9 Q. Luo, H. Zhang, J. Chen, D. You, C. Sun and Y. Zhang, *J. Membr. Sci.*, 2008, **325**, 553–558.
10 X. Teng, Y. Zhao, J. Xi, Z. Wu, X. Qiu and L. Chen, *J. Power Sources*, 2009, **189**, 1240–1246.
11 C. Jia, J. Liu and C. Yan, *J. Power Sources*, 2010, **195**, 4380–4383.
12 C. Sun, J. Chen, H. Zhang, X. Han and Q. Luo, *J. Power Sources*, 2010, **195**, 890–897.

13 B. Schwenzer, J. Zhang, S. Kim, L. Li, J. Liu and Z. Yang, *ChemSusChem*, 2011, **4**, 1388–1406.
14 W. Wang, Q. Luo, B. Li, X. Wei, L. Li and Z. Yang, *Adv. Funct. Mater.*, 2013, **23**, 970–986.
15 P. Zhao, H. Zhang, H. Zhou, J. Chen, S. Gao and B. Yi, *J. Power Sources*, 2006, **162**, 1416–1420.
16 D. Chen, S. Wang, M. Xiao and Y. Meng, *Energy Environ. Sci.*, 2010, **3**, 622–628.
17 D. Chen and M. A. Hickner, *Phys. Chem. Chem. Phys.*, 2013, **15**, 11299–11305.
18 C. Fujimoto, S. Kim, R. Stains, X. Wei, L. Li and Z. G. Yang, *Electrochem. Commun.*, 2012, **20**, 48–51.
19 T. H. Yu, Y. Sha, W.-G. Liu, B. V. Merinov, P. Shirvanian and W. A. Goddard, *J. Am. Chem. Soc.*, 2011, **133**, 19857–19863.
20 S. Kim, T. B. Tighe, B. Schwenzer, J. Yan, J. Zhang, J. Liu, Z. Yang and M. A. Hickner, *J. Appl. Electrochem.*, 2011, **41**, 1201–1213.
21 K. Grjotheim, F. Grönvold and J. Krogh-Moe, *J. Am. Chem. Soc.*, 1955, **77**, 5824–5827.
22 T. L. Ho, *Res. Chem. Intermed.*, 1989, **11**, 157–224.
23 Z. Mai, H. Zhang, H. Zhang, W. Xu, W. Wei, H. Na and X. Li, *ChemSusChem*, 2013, **6**, 328–335.
24 M. Vijayakumar, M. S. Bhuvaneswari, P. Nachimuthu, B. Schwenzer, S. Kim, Z. Yang, J. Liu, G. L. Graff, S. Thevuthasan and J. Hu, *J. Membr. Sci.*, 2011, **366**, 325–334.
25 J. S. Lawton, D. S. Aaron, Z. Tang and T. A. Zawodzinski, *J. Membr. Sci.*, 2013, **428**, 38–45.
26 S. J. Zaidi, S. Mikhailenko, G. Robertson, M. Guiver and S. Kaliaguine, *J. Membr. Sci.*, 2000, **173**, 17–34.
27 G. P. Robertson, S. D. Mikhailenko, K. Wang, P. Xing, M. D. Guiver and S. Kaliaguine, *J. Membr. Sci.*, 2003, **219**, 113–121.
28 Z. Mai, H. Zhang, X. Li, C. Bi and H. Dai, *J. Power Sources*, 2011, **196**, 482–487.